This full text paper was peer reviewed at the direction of IEEE Communications Society subject matter experts for publication in the WCNC 2008 proceedings.

Decoding on Graphs: LDPC-Coded MISO Systems and Belief Propagation

Amir H. Djahanshahi, Paul H. Siegel, and Larry B. Milstein

Department of Electrical and Computer Engineering
University of California, San Diego
Email: (adjahans, psiegel, and lmilstein)@ucsd.edu

***Abstract*— This paper proposes a new approach for decoding LDPC codes over MISO channels. Since in an $n_T \times 1$ MISO system with a modulation of alphabet size 2^M, n_T transmitted symbols are combined and produce one received symbol at the receiver, we propose considering the LDPC-coded MISO system as an LDPC code over 2^{Mn_T}-ary alphabet. Consequently, we propose a modified Tanner graph to introduce belief propagation for decoding MISO-LDPC systems. As a result, the MISO symbol detection and binary LDPC decoding steps are merged into a single message passing decoding. We also propose an efficient method that significantly reduces the complexity of belief propagation decoding in MISO-LDPC systems. Furthermore, we show that our proposed decoder outperforms the conventional decoder for short length LDPC codes in unknown channel scenarios.**

I. Introduction

Due to the increasing demand for multimedia data transmission in wireless mobile systems, there is an evident need for increasing the spectral efficiency of cellular systems. With their high spectral efficiency, MISO (multiple-input single-output) systems appear to be a crucial part of future cellular systems. Moreover, spatial diversity obtained by multiple transmit antennas is often indispensable for mitigation of the effects of the fading in wireless channels [1].

LDPC (low-density parity-check) codes are known for their superb error correction performance [2], [3]. With their near capacity performance [4], LDPC codes are among the most promising forward error correction schemes for wireless systems.

In this research, we propose a new scheme for joint detection and decoding of LDPC-coded MISO systems. Joint detection and decoding in MIMO-LDPC[1] systems, using a turbo architecture, has been studied in several papers (such as [5], [6]). They considered the MIMO symbol detector as the first decoder component of the turbo architecture and the LDPC decoder as the second decoder component. We consider this scheme as a reference for our comparisons and refer to it as the *turbo-type* receiver.

For the purpose of improving performance, we propose a new scheme for joint detection and decoding, which is based on considering the MISO-LDPC system as a 2^{Mn_T}-ary LDPC code, an LDPC code over 2^{Mn_T}-ary alphabet. We treat the received bits as a single symbol, then consider the whole system as a 2^{Mn_T}-ary LDPC code. We also introduce a modified Tanner graph that represents the MISO-LDPC system. It will be shown that BP (belief propagation) over the modified graph outperforms the traditional scheme in short length codes.

Considering the fact that straightforward implementation of BP (over the modified graph) is computationally intensive, we also propose a novel edge-based message passing (EBMP) algorithm that considerably reduces the decoding complexity.

In most practical scenarios, channel state information is not available at the receiver. Therefore, we also explore the unknown channel scenario. In particular, we examine the EM algorithm as a technique to iteratively estimate the channel and data. It will be shown that, in this case, the proposed scheme outperforms the existing scheme for short length codes.

The rest of this paper is organized as follows. Section II outlines the system model. In Section III a three-layer Tanner graph is introduced to exploit the BP algorithm for decoding in turbo-type receivers. To eliminate the positive feedback due to length-4 loops in the three-layer Tanner graphs, Section IV proposes a novel graph-based representation and a BP algorithm for decoding MISO-LDPC systems. Section V establishes a low-complexity implementation of the BP decoding over the modified graphs. Performance analysis and numerical comparisons are presented in Sections VI and VII, and Section VIII concludes the paper.

II. Problem Formulation

A. System Model

We consider the standard MISO-LDPC system model, i.e.,

$$y^{(k)} = \sqrt{\frac{E_s}{n_T}}\mathbf{C}^{(k)}\mathbf{x}^{(k)} + n^{(k)}, \tag{1}$$

where n_T is the number of transmit antennas and E_s represents the transmitted energy. Here, $y^{(k)}$ is the received symbol, $\mathbf{C}^{(k)}$ is the $1 \times n_T$ channel vector at the k^{th} time instant, $n^{(k)}$ is a sample of Gaussian noise with zero mean and variance Σ_n, and $\mathbf{x}^{(k)}$ is an $n_T \times 1$ vector of transmitted symbols at the

Acknowledgement: This research was partially supported by the Center for Wireless Communications at UCSD, and by the U.C. Discovery program.

[1]Note that MISO-LDPC is a special case of MIMO-LDPC.

k^{th} time instant, that contains n_T consecutive symbols of the LDPC codeword, i.e.,

$$\mathbf{x}^{(k)} = [\mathrm{x}_1^{(k)} \quad \mathrm{x}_2^{(k)} \quad \dots \quad \mathrm{x}_{n_T}^{(k)}]^T. \tag{2}$$

In (2), $\mathrm{x}_j^{(k)}$ (for $1 \le j \le n_T$) is a member of the alphabet $\mathbb{X}$, and corresponds to M consecutive LDPC bits, i.e.,

$$\mathrm{x}_j^{(k)} = \mathcal{F}\left(x_{(k-1)Mn_T+(j-1)M+1}, \dots, x_{(k-1)Mn_T+jM}\right), \tag{3}$$

where x_l (for $1 \le l \le N$) is the l^{th} bit of an (N, K) LDPC codeword, and $\mathcal{F}$ represents the modulation.

We consider a quasi-static Rayleigh flat fading channel model, where the channel remains constant during each fading block and changes independently from block to block (the block length is equal to the coherence time of the channel). Two different cases are considered for the channel: channel known at the receiver and channel unknown at the receiver.

1) Channel Known at the Receiver: Data detection when the channel is known at the receiver is straightforward. Since the channel is known, we can calculate the apriori probabilities and initialize the BP algorithm.

2) Channel Unknown at the Receiver: When the channel is not known at the receiver, it should first be estimated before data detection can take place. This is the idea behind pilot symbol assisted modulation. A set of pilot symbols, $\mathbf{p}$, is transmitted at the beginning of each block, the receiver estimates the channel based on the known pilot symbols, and then it decodes the received codeword using the estimated channel.

To unify the equations in the unknown channel case, (similar to [7]) we define:

$$\begin{aligned} \mathbf{X}_l &= [\mathbf{p} \quad \mathbf{x}^{(ln_D+1)} \quad \dots \quad \mathbf{x}^{((l+1)n_D)}] \\ \mathbf{Y}_l &= [y_p^{(l)} \quad y^{(ln_D+1)} \quad \dots \quad y^{((l+1)n_D)}] \\ \mathbf{N}_l &= [n_p^{(l)} \quad n^{(ln_D+1)} \quad \dots \quad n^{((l+1)n_D)}], \end{aligned} \tag{4}$$

where $\mathbf{p}$ is an $n_T \times n_P$ matrix containing the pilot symbols and $\mathbf{X}_l$ is the $n_T \times (n_P + n_D)$ matrix of transmitted (pilot and data) symbols at the l^{th} block (each block contains $n_P + n_D$ MISO symbols). $\mathbf{Y}_l$ and $\mathbf{N}_l$ are $1 \times (n_P + n_D)$ vectors of received symbols and noise samples at the l^{th} block, respectively. Furthermore, $\mathbf{y}_p^{(l)}$ and $n_p^{(l)}$ are $1 \times n_P$ vectors containing the received signals due to the pilot symbols and Gaussian noise samples at the first n_P time instants of the l^{th} block, respectively. One can easily show that

$$\mathbf{Y}_l = \sqrt{\frac{E_s}{n_T}}\mathbf{C}_l\mathbf{X}_l + \mathbf{N}_l, \tag{5}$$

where $\mathbf{C}_l$ is the $1 \times n_T$ channel vector at the l^{th} block.

It has been shown that a turbo-EM estimator with the ability to use the soft output of the decoder outperforms the conventional MMSE-based channel estimator [8], [9]. So, we will use the EM algorithm for joint estimation and detection in the unknown channel case.

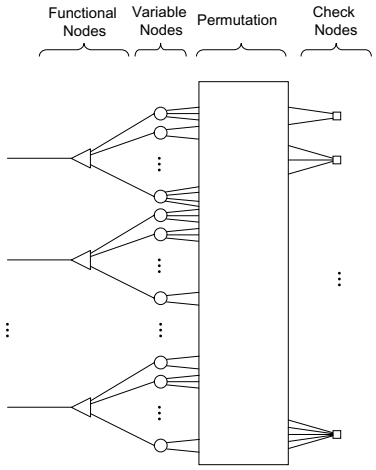

Fig. 1. A three-layer Tanner graph

B. EM Algorithm

After some manipulations, the EM update equations can be written as follows (similar to [5]):

$$\mathbf{C}_l^i = \mathbf{Y}_l\mathbf{U}_l^H\mathbf{R}_l^{-1}, \tag{6}$$

where $\mathbf{C}_l^i$ is the i^{th} estimation of $\mathbf{C}_l$. Here $\mathbf{R}_l = E_{\mathbf{X}_l|\mathbf{C}_l^i,\mathbf{Y}_l}\left[\mathbf{X}_l\mathbf{X}_l^H\right]$ and $\mathbf{U}_l = E_{\mathbf{X}_l|\mathbf{C}_l^i,\mathbf{Y}_l}\left[\mathbf{X}_l\right]$. Note that $\mathbf{R}_l$ and $\mathbf{U}_l$ are computed using the soft output of the LDPC decoder.

The EM algorithm always converges, but not necessarily to the global maximum. To avoid the possibility of converging to a local maximum, the initial conditions should be chosen with care to ensure that the global maximum is reached. Hence we use the output of the PSAM (Pilot Symbol Assisted Modulation) estimator to estimate the channel.

III. Graph Based Representation of Turbo-type Receiver

To exploit message passing algorithms for decoding in "turbo type" receivers, (similar to [10]) we construct a three-layer Tanner graph (see Fig. 1), where the second and third layers are, respectively, variable and check nodes of the LDPC code. The first layer consists of some "generalized nodes" which we call *functional nodes* and represent by triangles in the Tanner graph. Functional nodes represent the MISO symbol detectors in the turbo-type receiver. Each functional node is connected to Mn_T consecutive LDPC variable nodes from the second layer of the graph.

It can be shown that decoding with turbo-type receiver, is formally identical to BP over a three-layer Tanner graph (see [11], [12] for the proof). Furthermore one can easily see that appending the functional nodes to the bipartite graph of the LDPC code (with high probability) introduces a number of length-4 loops. Thus, BP over the three-layer Tanner graph (or turbo-type receiver) would suffer from positive feedback. To address this problem, a modified Tanner graph would be introduced to represent MISO-LDPC systems. It can be shown that BP over the modified graph eliminates the length-4 loops problem [11], [12].

IV. Modified Tanner Graphs

Similar to binary LDPC codes, a modified parity check matrix and a Tanner graph can be defined for 2^{Mn_T}-ary LDPC codes. As in the binary LDPC graph, each column of the modified parity check matrix represents a modified variable node. Since variable nodes in a 2^{Mn_T}-ary LDPC code correspond to Mn_T consecutive variable nodes in the original graph, each column of the modified parity check matrix represents Mn_T consecutive columns of the original parity check matrix. To derive the modified parity check matrix, we consider each Mn_T consecutive components in each row of the original parity check matrix as a binary word of length Mn_T, then calculate the equivalent 2^{Mn_T}-ary value to determine the corresponding component in the modified matrix.

The modified parity check matrix can be used to define the modified Tanner graph. Each Tanner graph has three parts: variable nodes, check nodes, and the edges connecting the variable nodes to the check nodes. In order to derive the modified Tanner graph, we define how each of the three above mentioned parts are affected.

Variable nodes in the modified Tanner graph correspond to Mn_T consecutive variable nodes in the original Tanner graph, hence the number of variable nodes is $\frac{1}{Mn_T}$ times the number of the variable nodes in the original graph.

Given that each check node represents one constraint in the LDPC code, the number of check nodes is not affected by modifying the graph. However, check nodes in the modified graph are connected to 2^{Mn_T}-ary variable nodes instead of binary variable nodes.

If any of the Mn_T binary constituent variable nodes of a 2^{Mn_T}-ary modified variable node are connected to a check node (in the original graph), there would be an edge connecting the 2^{Mn_T}-ary variable node to the corresponding modified check node (in the modified graph).

In the modified Tanner graph, the edges are not all identical. To differentiate the edges in the modified Tanner graph, we label them with the corresponding component in the modified parity check matrix. Example 1 sheds light on the procedure of deriving the modified parity check matrix and Tanner graph.

Example 1: Deriving the modified parity check matrix and Tanner graph from the binary parity check matrix when $Mn_T = 2$:

Consider the following binary parity check matrix:

$$\mathbf{H} = \begin{pmatrix} 1 & 0 & 0 & 1 & 1 & 0 & 1 & 0 \\ 1 & 1 & 0 & 0 & 0 & 1 & 0 & 0 \\ 0 & 0 & 1 & 0 & 1 & 0 & 0 & 1 \\ 0 & 0 & 1 & 1 & 0 & 1 & 0 & 0 \end{pmatrix}. \tag{7}$$

To derive the modified parity check matrix (when $Mn_T = 2$), we combine every two consecutive columns in the original parity check matrix and consider them as a column in the modified parity check matrix. For example, the first two columns of the first row of the binary parity check matrix are 10, so there should be a value of 2 in the first row and first column of the modified parity check matrix.

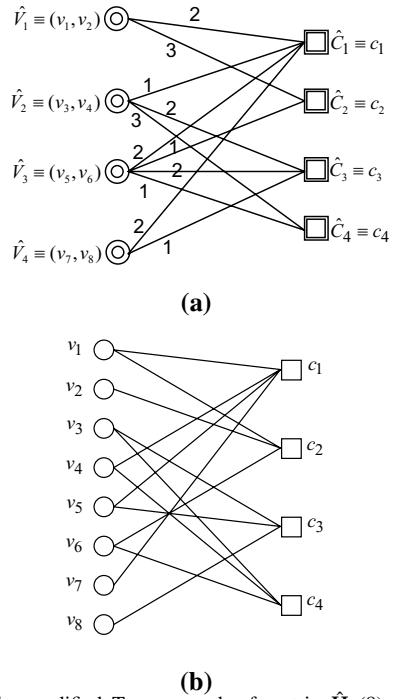

Fig. 2. **(a)** The modified Tanner graph of matrix $\hat{\mathbf{H}}$ (8), **(b)** The binary Tanner graph corresponding to $\mathbf{H}$ (7).

Following the same procedure, the rest of the quaternary parity check matrix can be obtained.

$$\hat{\mathbf{H}} = \begin{pmatrix} 2 & 1 & 2 & 2 \\ 3 & 0 & 1 & 0 \\ 0 & 2 & 2 & 1 \\ 0 & 3 & 1 & 0 \end{pmatrix}. \tag{8}$$

Fig. 2.(a) represents the modified Tanner graph corresponding to $\hat{\mathbf{H}}$. Each quaternary variable node in this graph represents two consecutive variable nodes in the original Tanner graph. For example, $\hat{V}_1$ corresponds to v_1 and v_2 in the original binary graph (Fig. 2.(b)).

Check nodes in the modified graph represent the same constraints as in the orginal graph. To determine the constraint imposed by a check node, we write the corresponding values for the variable nodes and edges as a binary vector of length two, then we use the inner product and summation over GF(2) to determine the constraint. For example, $\hat{C}_1$ implies

$$\begin{aligned} &< 2, \mathbf{x}^{(1)} > + < 1, \mathbf{x}^{(2)} > + < 2, \mathbf{x}^{(3)} > + \\ &< 2, \mathbf{x}^{(4)} >= 0 \qquad \text{modulo } 2, \end{aligned} \tag{9}$$

where $< ., . >$ represents the inner-product operator over $GF(2)$. Equation (9) can be rewritten as

$$\begin{aligned} &[1 \quad 0]. \begin{bmatrix} x_1 \\ x_2 \end{bmatrix} + [0 \quad 1]. \begin{bmatrix} x_3 \\ x_4 \end{bmatrix} + [1 \quad 0]. \begin{bmatrix} x_5 \\ x_6 \end{bmatrix} + \\ &[1 \quad 0]. \begin{bmatrix} x_7 \\ x_8 \end{bmatrix} = 0 \qquad \text{modulo } 2, \end{aligned} \tag{10}$$

Or, equivalently,

$$x_1 + x_4 + x_5 + x_7 = 0 \qquad \text{modulo } 2, \tag{11}$$

which is the same as the constraint imposed by the first row of $\mathbf{H}$, (7).

A. BP over Modified Tanner Graphs

BP over modified Tanner graphs is similar to BP over binary graphs. The only difference is that in the modified graph nodes compute the probability of 2^{Mn_T} possible cases instead of just one log-likelihood ratio (LLR) value. To be more specific, in a modified Tanner graph, each node at each iteration computes 2^{Mn_T} messages regarding the probability of each possible case.

Similar to [13], we define the following parameters which we will use in BP:

Definition 1: $f_{\mathbf{s}}^{(k)}$ denotes the conditional probability that the k^{th} modified variable node is $\mathbf{s} \in \{0,1\}^{Mn_T}$, given $\mathbf{y}^{(k)}$.

Definition 2: $q_{\mathbf{s}}^{(nm)}$ denotes the message sent from the n^{th} modified variable node to the m^{th} modified check node, and represents an estimate of the probability that the n^{th} modified variable node is $\mathbf{s}$.

Definition 3: $r_{\mathbf{s}}^{(mn)}$ denotes the message sent from the m^{th} modified check node to the n^{th} modified variable node, and represents an estimate of the probability that the n^{th} modified variable node is $\mathbf{s}$.

Definition 4: $N(m)$ denotes the subset of the modified variable nodes participating in the m^{th} check equation.

Definition 5: $M(n)$ denotes the subset of the check nodes depending on the n^{th} modified variable node.

Definition 6: $\mathbb{S}^m$ denotes the m^{th} check-node local-codewords, where m^{th} check-node local-codewords, in a modified $(\lceil \frac{N}{Mn_T} \rceil , \lceil \frac{K}{Mn_T} \rceil)$ LDPC code, are the 2^{Mn_T}-ary length-$\lceil \frac{N}{Mn_T} \rceil$ vectors that satisfy the m^{th} check equation.

Definition 7: $\mathbb{S}_{\mathbf{s}}^{mn}$ denotes the subset of the m^{th} check-node local-codewords, whose n^{th} element is $\mathbf{s}$.

The derivation of the BP equations over modified Tanner graphs is similar to the derivation of the BP equations of LDPC codes over $GF(Q)$ [13], and due to the lack of space is omitted (see [11], [12] for details).

B. Initialization

Similar to LDPC codes over $GF(Q)$ [13], the probability of each possible case given the received codeword is used to initialize the BP algorithm. It can be shown that [11], [12]

$$f_{\mathbf{s}}^{(k)} = \frac{\alpha^{(k)}}{\sqrt{2\pi\Sigma_{\mathbf{n}}}} e^{-\left[\left(y^{(k)}-\mathbf{C}^{(k)}G(\mathbf{s})\right)^{*}\Sigma_{\mathbf{n}}^{-1}\left(y^{(k)}-\mathbf{C}^{(k)}G(\mathbf{s})\right)\right]}, \quad (12)$$

where $\alpha^{(k)}$ is chosen to ensure $\sum_{\mathbf{s}} f_{\mathbf{s}}^{(k)} = 1$, * is the complex conjugate operator, and $G(\mathbf{s})$, an $n_T \times 1$ vector, is given by

$$G(\mathbf{s}) = [\mathcal{F}(s_1,\ldots,s_M) \ \ \ldots \ \ \mathcal{F}(s_{M(n_T-1)+1},\ldots,s_{Mn_T})]^T,$$

where s_l (for $1 \le l \le Mn_T$) is the l^{th} element of vector $\mathbf{s} \in \{0,1\}^{Mn_T}$.

C. Variable-to-Check Node Messages

The variable-to-check message, $q_{\mathbf{s}}^{(nm)}$, for BP can be computed using [11], [12]:

$$q_{\mathbf{s}}^{(nm)} = \beta^{(nm)} f_{\mathbf{s}}^{(n)} \prod_{j \in M(n)\setminus m} r_{\mathbf{s}}^{(jn)}, \quad (13)$$

where $\beta^{(nm)}$ is a normalization factor chosen to ensure that $\sum_{\mathbf{s}} q_{\mathbf{s}}^{(nm)} = 1$.

Tentative decoding for the n^{th} bit can be done as follows:

$$\hat{x}_l = \arg\max_{d} \sum_{\mathbf{s} \in \mathbb{D}_d^{(\mathtt{mod}(l-1,Mn_T)+1)}} f_{\mathbf{s}}^{(\lceil \frac{l}{Mn_T} \rceil)} \prod_{j \in M(l)} r_{\mathbf{s}}^{(j,\lceil \frac{l}{Mn_T} \rceil)}, \quad (14)$$

where $d \in \{0,1\}$, and $\mathbb{D}_d^{(i)}$ is the set of all length-Mn_T binary vectors whose i^{th} bit is d, and $\mathtt{mod}(l-1, Mn_T)$ represents the reminder of the division of $l-1$ by Mn_T.

D. Check-to-Variable Node Messages

The check-to-variable message, $r_{\mathbf{s}}^{(mn)}$, can be calculated as follows [11], [12]:

$$r_{\mathbf{s}}^{(mn)} = \gamma^{(mn)} \sum_{\mathbf{X}' \in \mathbb{S}_{\mathbf{s}}^{mn}} \prod_{j \in N(m)\setminus n} q_{\mathbf{x}'_j}^{(jm)}, \quad (15)$$

where $\mathbf{x}'_j$ is the jth element of $\mathbf{X}'$, and $\gamma^{(mn)}$ is a constant that ensures $\sum_{\mathbf{s}} r_{\mathbf{s}}^{(mn)} = 1$.

V. Edge-Based Message Passing for Modified Tanner Graphs

A straightforward implementation of the BP is computationally extensive. Using the LLR of the edges as messages, we propose an alternative algorithm for implementation of BP that considerably reduces the complexity of the decoding.

Consider the following definitions of parameters that we will use in the EBMP algorithm:

Definition 8: $\mathbb{Z}_{\mathbf{s}}$ denotes the subset of 2^{Mn_T}-ary symbols $\mathbf{u} \in \{0,1\}^{Mn_T}$, such that $< \mathbf{s}, \mathbf{u} >= 0$, i.e.,

$$\mathbb{Z}_{\mathbf{s}} \triangleq \{\mathbf{u} | < \mathbf{s}, \mathbf{u} >= 0\}. \quad (16)$$

Definition 9: $\mathbb{O}_{\mathbf{s}}$ denotes the subset of 2^{Mn_T}-ary symbols $\mathbf{u} \in \{0,1\}^{Mn_T}$, such that $< \mathbf{s}, \mathbf{u} >= 1$, i.e.,

$$\mathbb{O}_{\mathbf{s}} \triangleq \{\mathbf{u} | < \mathbf{s}, \mathbf{u} >= 1\}. \quad (17)$$

Definition 10: $l(e)$ denotes the LLR of edge e, and is given by

$$l(e) \triangleq \ln \frac{\sum_{\mathbf{s} \in \mathbb{Z}_\lambda} P(\hat{V}_n = \mathbf{s})}{\sum_{\mathbf{s} \in \mathbb{O}_\lambda} P(\hat{V}_n = \mathbf{s})}, \quad (18)$$

where $\hat{V}_n$ is the modified variable node connected to e, and λ is the label of e in the modified Tanner graph.

With some algebraic manipulations, one can show that:

Theorem 1: The LLRs of the edges are sufficient for calculation of the variable-to-check messages in the BP algorithm

Theorem 2: The LLRs of the edges are sufficient for calculation of the check-to-variable messages in the BP algorithm

(see [11], [12] for the proof).

From Theorems 1 and 2, we deduce that the LLRs of the edges are sufficient for implementation of the update equations. Therefore we make the following definitions:

Definition 11: $q^{(nm)}$ denotes the message sent from the n^{th} modified variable node to the m^{th} modified check node, and

represents an estimate of the LLR of the edge connecting these nodes. i.e.,

$$q^{(nm)} \triangleq \ln \frac{\sum_{\mathbf{s}\in\mathbb{Z}_{\hat{\mathbf{H}}_{mn}}} q_{\mathbf{s}}^{(nm)}}{\sum_{\mathbf{s}\in\mathbb{O}_{\hat{\mathbf{H}}_{mn}}} q_{\mathbf{s}}^{(nm)}}. \tag{19}$$

Definition 12: $r^{(mn)}$ denotes the message sent from the m^{th} modified check node to the n^{th} modified variable node, and represents an estimate of the LLR of the edge connecting $\hat{V}_n$ to $\hat{C}_m$. i.e.,

$$r^{(mn)} \triangleq \ln \frac{\sum_{\mathbf{s}\in\mathbb{Z}_{\hat{\mathbf{H}}_{mn}}} r_{\mathbf{s}}^{(mn)}}{\sum_{\mathbf{s}\in\mathbb{O}_{\hat{\mathbf{H}}_{mn}}} r_{\mathbf{s}}^{(mn)}}. \tag{20}$$

Since $r_{\mathbf{s}}^{(mn)}$ is the same for all $\mathbf{s} \in \mathbb{Z}_{\hat{\mathbf{H}}_{mn}}$ and also for all $\mathbf{s} \in \mathbb{O}_{\hat{\mathbf{H}}_{mn}}$, $r^{(mn)}$ can be reformulated as

$$r^{(mn)} = \ln \frac{r_{\mathbf{s_1}}^{(mn)}}{r_{\mathbf{s_2}}^{(mn)}}, \qquad \text{for} \quad \mathbf{s}_1 \in \mathbb{Z}_{\hat{\mathbf{H}}_{mn}} \text{ and } \mathbf{s}_2 \in \mathbb{O}_{\hat{\mathbf{H}}_{mn}}. \tag{21}$$

According to Theorems 1 and 2, check and variable nodes can compute check-to-variable messages ($r_{\mathbf{s}}^{(mn)}$) and variable-to-check messages ($q_{\mathbf{s}}^{(nm)}$) with LLR messages($r^{(mn)}$ and $q^{(nm)}$) of the edges connected to them. Consequently, we introduce the EBMP algorithm where each node just passes the LLR messages. As a result the nodes just send *one* message for each edge, as opposed to the 2^{Mn_T} messages passed in the BP algorithm. The EBMP update equations can be formulated as follows. Due to the limited space, the derivations are omitted (see [11], [12] for details).

$$q^{(nm)} = \ln \frac{\sum_{\mathbf{s}\in\mathbb{Z}_{\hat{\mathbf{H}}_{mn}}} f_{\mathbf{s}}^{(n)} \exp\left[\sum_{\left\{j \,\middle|\, j\in M(n)\setminus m, <\hat{\mathbf{H}}_{jn},\mathbf{s}>=\mathbf{0}\right\}} r^{(jn)}\right]}{\sum_{\mathbf{s}\in\mathbb{O}_{\hat{\mathbf{H}}_{mn}}} f_{\mathbf{s}}^{(n)} \exp\left[\sum_{\left\{j \,\middle|\, j\in M(n)\setminus m, <\hat{\mathbf{H}}_{jn},\mathbf{s}>=\mathbf{0}\right\}} r^{(jn)}\right]}$$

$$r^{(mn)} = \ln \frac{1+\prod_{j\in N(m)\setminus n} \tanh\left[\frac{q^{(jm)}}{2}\right]}{1-\prod_{j\in N(m)\setminus n} \tanh\left[\frac{q^{(jm)}}{2}\right]}. \tag{22}$$

And the initialization can be done using

$$q^{(nm)} = \ln \frac{\sum_{\mathbf{s}\in\mathbb{Z}_{\hat{\mathbf{H}}_{mn}}} \mathbf{P}_{X|Y}\left(\mathbf{x}^{(n)} = \mathbf{s}|y^{(n)}\right)}{\sum_{\mathbf{s}\in\mathbb{O}_{\hat{\mathbf{H}}_{mn}}} \mathbf{P}_{X|Y}\left(\mathbf{x}^{(n)} = \mathbf{s}|y^{(n)}\right)}. \tag{23}$$

VI. Performance Analysis

When the modified LDPC graph is acyclic, the EBMP is equivalent to MAP [11], [12], and performs the same as or better than any other decoding scheme, such as the turbo-type decoder. To compare the performance of receivers over graphs with cycles (e.g. finite length LDPC codes), we consider two different scenarios:

- S_1: Any pair of variable nodes that are connected to a SISO-MISO (Soft-in Soft-out MISO) symbol detector, are not connected to the same check node.
- S_2: There exists at least one pair of variable nodes that are connected to a given SISO-MISO detector and a given check node.

It can be shown that both systems perform the same in the first scenario [11], [12]. However, it is a hard task to make a rigorous comparison between performance of algorithms in the second scenario. It is not hard to see that the pair of variable nodes, the check node, and the SISO-MISO detector connected to both variable nodes form a length-4 loop in the turbo-type decoder. However this loop does not appear in the modified graph. To be more specific, the length-4 loop would be transformed to an edge in the modified graph. Furthermore, one can easily see that each loop in the modified graph corresponds to a loop in the turbo-type architecture. Therefore conversion from a three-layer graph to the modified graph not only does not generate any new loops, but also eliminates the length-4 loops generated due to the turbo-type decoder. Therefore, due to the positive feedback, we expect the EBMP to outperform the turbo type scheme. We further expect the performance difference to depend on the ratio of the number of length-4 loops to the total number of loops in the turbo-type decoder.

VII. Numerical Results

We simulated our proposed algorithm for joint detection and decoding in a 2×1 MISO-LDPC system for both known and unknown channel cases. We analyzed a random (3,4)-regular LDPC code (with 4-cycles removed) of length $N = 252$. In all cases, we plot the bit error rate in terms of the $\frac{E_b}{N_0}$. Each plot compares the performance of the proposed (EBMP) algorithm with the turbo-type receiver. The comparisons all correspond to quasi-static Rayleigh fading channels. Unless explicitly mentioned, $T_c = 8T$ (T_c is the coherence time of the channel and T represents the symbol time), the modulation is 8-ary QAM with Gray labeling, i.e. $M = 3$, also the pilot symbols power is assumed to be 4 times the data symbols power.

Figure 3 illustrates the performance of receivers for both known and unknown channels. One can easily see that the proposed scheme outperforms the traditional scheme, turbo type receiver, in both scenarios. Moreover the performance difference in the unknown channel case is larger than the difference in the known channel scenario. The reason for this observation is that in the unknown channels, the MISO-SISO detectors are "weaker", i.e. get less information from the received symbols, and consequently generate more positive feedback, as opposed to the known channel scenario.

Figure 4 represents the effect of the coherence time of the channel on the performance of both systems over unknown channels. One can see that increasing the coherence time increases the performance difference of the systems. This might be due to the fact that channel estimation errors can be a more significant contributor to erroneous detection in fast fading channels.

Figure 5 investigates the effects of the pilot symbols power on the performance of the systems in the unknown channel cases. By increasing the pilot symbols power, the performance difference becomes closer to the known channel case.

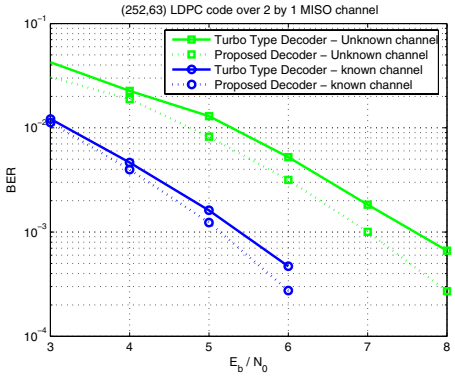

Fig. 3. BER vs. E_b/N_0 for known and unknown channel scenarios

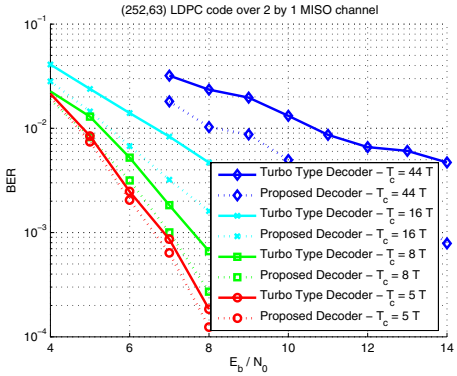

Fig. 4. BER vs. E_b/N_0 for various channel coherent times

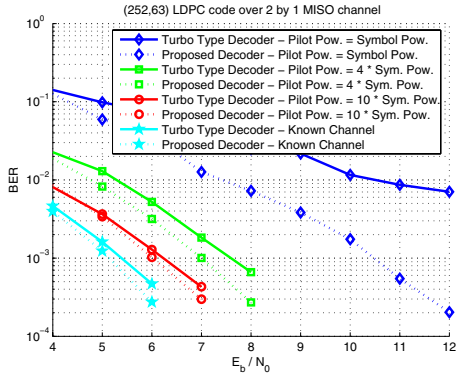

Fig. 5. BER vs. E_b/N_0 for different pilot symbols powers

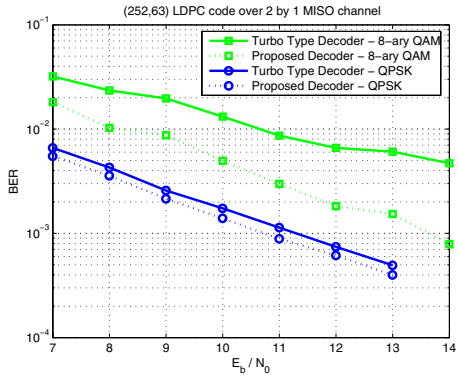

Fig. 6. BER vs. E_b/N_0 for 8-ary QAM and QPSK modulations

Finally, Figure 6 demonstrates the effects of the modulation size on the performance of systems over unknown slow fading channels. One can see that increasing the modulation size increases the performance gap between both systems. This is due to the fact that by increasing the modulation size, the number of length-4 loops in the turbo-type structure increases.

Additional simulation results (not shown here) indicate that more significant performance gains can be obtained with irregular LDPC codes, which is due to the fact that the three-layer graphs of (finite length) irregular LDPC codes contain more length-4 loops than those of regular LDPC codes.

VIII. Concluding Remarks

In this paper, we introduced a new graph-based representation of MISO-LDPC systems which can be used for joint MISO-symbol detection and decoding using message passing algorithms. We presented a novel edge-based message passing algorithm for implementation of BP that considerably decreases the computational complexity of the BP algorithm. To characterize the performance of the turbo-type receiver, we introduced a three-layer Tanner graph. We noted that on acyclic modified graphs, our algorithm is equivalent to MAP decoding. Moreover, in graphs with cycles, we identified scenarios where both algorithms perform the same. Our simulation results show that for short length LDPC codes the proposed algorithm outperforms the traditional one in the unknown channel scenarios.

References

[1] T. Wang, Y. Yao, and G. B. Giannakis, "Non-coherent distributed space-time processing for multiuser cooperative transmissions," *IEEE Transactions on Wireless Communications*, vol. 5, pp. 3339–43, December 2006.

[2] R. G. Gallager, *Low Density Parity Check Codes*, Monograph, M.I.T. Press, 1963.

[3] D. J. C. MacKay, "Good error-correcting codes based on very sparse matrices," *IEEE Transactions on Information Theory*, vol. 45, pp. 399431, 1999.

[4] D. J. C. MacKay and R.M.Neal, "Near Shannon limit performance of low density parity check codes," *Electronic Letters*, vol. 32, no. 18, pp. 1645–46, 1996.

[5] J. Zheng, B. D. Rao, "LDPC-coded MIMO systems with unknown block fading channels: soft MIMO detector design, channel estimation, and code optimization," *IEEE Transactions on Signal Processing*, vol. 54, no. 4, pp. 1504–18, 2006.

[6] S. ten Brink, G. Kramer, and A. Ashikhmin, "Design of low-density parity-check codes for modulation and detection," *IEEE Transactions on Communications*, vol. 52, pp. 670–78, 2004.

[7] M. Fozunbal, S. W. McLaughlin, R. W. Schafer, and J. M. Landsberg, "On space-time coding in the presence of spatio-temporal correlation," *IEEE Transactions on Information Theory*, vol. 50, no. 9, 2004.

[8] M. Gonzalez-Lopez, J. Miguez, and L. Castedo, "Turbo aided maximum likelihood channel estimation for space time systems," *proc. IEEE Int. Symp. Spread Spectrum Techniques and Applications*, vol. 1, no. 6, pp. 123–126, 2000.

[9] H. Wymeersch, F. Simoens, and M. Moeneclaey, "Code-aided joint channel estimation and frame synchronization for MIMO systems," *Workshop on Signal Processing Advances in Wireless Communications (SPAWC04)*, 2004.

[10] B. M. Kurkoski, P. H. Siegel, and J. K. Wolf, "Joint message-passing decoding of LDPC Codes and partial-response channels," *IEEE Transactions on Information Theory*, vol. 48, no. 6, pp. 1410–22, 2002.

[11] A. H. Djahanshahi, *Joint equalization and decoding of graph-based codes in multiple-antenna systems*, PhD Thesis, University of California - San Diego, in preparation.

[12] http://ieng9.ucsd.edu/∼adjahans/publications/MIMOLDPC.pdf.

[13] Davey, MacKay, "Low density parity check codes over GF(Q)," *IEEE Comm. Letters*, vol. 2, no. 6, pp. 165–167, 1998.